Relation between usage of dating apps and sexually transmitted infections

Carlos Bustamante[1], Jordan Lyerla[2], Aaron Martin[1], Fabio Milner[1], Elisha Smith[3], and Josean Velazquez[1]

[1]Arizona State University
[2]University of Kansas
[3]Kean University

July 21, 2023

Keywords: sexually transmitted infections, dating apps, sex

Abstract

In the United States, incidence of sexually transmitted infections (STIs) has risen sharply. Between 2014 and 2019, male and female incidence has increased 62.8% and 21.4%, respectively, with an estimated 68 million Americans contracting an STI in 2018 [7]. Some human behaviors impacting the STI epidemic are unprotected sex and multiple sexual partners [23]. Increasing dating app usage has been postulated as a driver for the increase in these behaviors. This study attempts to quantify the impact of dating apps on the incidence and prevalence of STIs utilizing a sex-structured SIS model of STI transmission. The model is also used to assess the possible benefit of in-app prevention campaigns. Additionally, the mathematical model is used to estimate the percentage of people who seek treatment after contracting an STI.

2014-2019, male and female incidence has increased 62.8

1 Introduction

Sexually transmitted infections (STIs), also referred to as sexually transmitted diseases (STDs), are very widespread in the U.S. and cause many short- and long-term health problems as well as great expenses to treat them. The Center for Disease Control and Prevention's (CDC) latest estimates indicate that 68 million people (20% of the U.S. population) – approximately one in five people – had an STI on any given day in 2018, with 25 million of them newly acquired that year, and these cost the American healthcare system nearly $16 billion in direct medical costs alone [7].

The eight most common STIs are chlamydia, gonorrhea, syphilis, trichomoniasis, hepatitis B virus (HBV), herpes simplex virus type 2 (HSV-2), human immunedeficiency virus (HIV), and human papilloma virus (HPV). The first three are caused by bacteria, the fourth one by protozoa, and are generally curable with existing single-dose regimens of antibiotics lasting 1-4 weeks. The last four are viral infections for the first three of which the best available treatments are antivirals and, for HPV, there is no treatment but there are preventative vaccines [26]. Table 1 summarizes their nationwide prevalence and incidence in 2018 [7].

Table 2 contains more detailed prevalence data for the same year, such as the Q1, Q2, and Q3 values for each prevalence that refer to the 25th, 50th, and 75th percentiles respectively. This data confirms that chlamydia and gonorrhea have the highest incidence and prevalence rates and, as such, have a significant impact on the increasing STI rates in the United States. [25]

One recent social change that has been postulated to modify human sexual behavior, and in turn the incidence and prevalence of STIs, is the advent of dating apps. For context, mobile phone and dating site applications have seen a global surge in usage since the start of COVID-19. For example, in the

STI	Prevalence (in millions)	Incidence (in millions)
Chlamydia	2.4	4
Gonorrhea	0.209	1.6
Syphilis	0.156	0.146
Trichomoniasis	2.6	6.9
HBV	0.103	0.0083
HSV-2	18.6	0.572
HIV	0.984	0.0326
HPV	42.5	13

Table 1: Prevalence and Incidence of the 8 most common STIs, U.S. 2018

	Men, Median (25th–75th Percentile)†	Women, Median (25th–75th Percentile)†	Total, Median (25th–75th Percentile)†,‡
All ages§			
Chlamydia	1,050,000 (944,000–1,157,000)	1,306,000 (1,193,000–1,418,000)	2,353,000 (2,202,000–2,508,000)
Gonorrhea	50,000 (40,000–63,000)	155,000 (131,000–184,000)	209,000 (183,000–241,000)
AMR gonorrhea¶	26,000 (21,000–32,000)	80,000 (67,000–94,000)	107,000 (94,000–124,000)
Trichomoniasis	470,000 (414,000–530,000)	2,103,000 (1,982,000–2,225,000)	2,576,000 (2,446,000–2,713,000)
Syphilis	112,000 (92,000–137,000)	38,000 (28,000–55,000)	156,000 (132,000–184,000)
Genital herpes‖	6,354,000 (6,093,000–6,629,000)	12,203,000 (11,885,000–12,538,000)	18,574,000 (18,140,000–19,002,000)
HPV**	23,411,000 (22,669,000–24,200,000)	19,210,000 (18,700,000–19,776,000)	42,500,000 (41,400,000–43,700,000)
HBV††	51,000 (41,000–61,000)	52,000 (42,000–63,000)	103,000 (89,000–118,000)
HIV††	775,600 (769,200–781,900)	208,400 (205,600–211,200)	984,000 (977,000–990,900)
Total‡	32,321,000 (31,519,000–33,124,000)	35,311,000 (34,656,000–35,980,000)	67,636,000 (66,599,000–68,668,000)
Ages 15–24 y			
Chlamydia	595,000 (530,000–659,000)	990,000 (899,000–1,084,000)	1,583,000 (1,472,000–1,696,000)
Gonorrhea	20,000 (15,000–27,000)	90,000 (72,000–115,000)	113,000 (93,000–138,000)
AMR gonorrhea¶	10,000 (8,000–14,000)	46,000 (37,000–59,000)	58,000 (48,000–71,000)
Trichomoniasis	83,000 (63,000–107,000)‡‡	314,000 (275,000–356,000)	402,000 (356,000–449,000)
Syphilis	24,000 (18,000–32,000)	10,000 (7,000–16,000)	36,000 (29,000–46,000)
Genital herpes‖	398,000 (336,000–472,000)	918,000 (823,000–1,017,000)	1,325,000 (1,208,000–1,447,000)
HPV**	3,604,000 (3,383,000–3,826,000)	5,376,000 (5,091,000–5,645,000)	8,979,000 (8,625,000–9,500,000)
HBV††	NC	NC	NC
HIV††,§§	39,900 (38,200–41,500)	5500 (4900–6000)	45,400 (43,600–47,100)
Total‡	4,829,000 (4,587,000–5,062,000)	7,779,000 (7,467,000–8,096,000)	12,608,000 (12,219,000–12,988,000)

Table 2: Estimated number of prevalent sexually transmitted infections. United States, 2018

first quarter of 2022, 39% of all single, divorced, or widowed consumers reported use of an online dating site in the previous month [21]. This trend in human dating behavior is consistent with the recorded 17 million daily users among the top twenty dating apps in 2020[17]. This data is further corroborated by statistics that state 26.6 million Americans used a smartphone dating app in 2020, with Tinder reporting 957,700 downloads in the month of June 2022 alone [9].

Researchers from The Chicago School of Professional Psychology, found a relationship between sexual discounting, usage of dating applications, and sexual risk. Delay discounting refers to the devaluation of an objective as a function of increasing time; correspondingly, sexual discounting indicates the devaluation of protected sex in favor of unprotected, immediate sex. The researchers utilized Kendall's τ-b to calculate the correlation between risky sexual behavior and sexual discounting for dating app users and non-users. Their results give evidence of a strong correlation among users ($r = -0.357$) and no correlation among dating app non-users ($r = -0.05$). This adds support to the hypothesis that dating apps may play a significant role in the increasing STI rates [4].

The relationship between risky sexual behavior and dating app usage is significant as such behaviors have been linked to the increased STI infection rates. Several critical risky sexual behaviors have been associated with dating app use: unprotected sex, multiple sexual partners, sex after too much to drink, and sex after using drugs. In a 2017-study to evaluate the correlation between these sexual risk behaviors and dating app usage, the authors surveyed 509 heterosexual, cisgender undergraduate students (18-25 years old) from a psychology class at a Mid-Atlantic institution. The survey evaluated the students' impulsivity, dating app usage and motivations, sexual behavior, and demographics. It was found that individuals who seek sexual partners through dating sites and apps have higher rates of unprotected sex, higher rates of STIs, and a greater number of sexual partners; the individuals who used dating apps were also found to be more impulsive [23].

The extant literature presents a qualitative correlation between dating app usage, sexual risk behavior, and STIs but fails to provide a quantitative assessment of the impact dating apps have on increasing STI incidence. As such, this study attempts to use SIS epidemic modeling in order to quantify the increase in STIs that has resulted from the use of dating apps. In order to use our SIS models, several types of data are needed to estimate model parameters. We found a scarcity or absemce of data needed, for example to estimate the percentage of people who seek treatment after contracting an STI, as STIs are often asymptomatic. To solve for this unknown value, we used used an algebraic relation among 8 parameters after obtaining the values for most of those from existing literature or parameter-fitting using our models.

To combat the rising STI rates, prevention campaigns within dating apps have been proposed as a possibility. In one study the authors performed in-depth interviews of 25 men who have sex with men to qualitatively assess the potential to deliver sexual health information and promotion through dating apps. Results indicate that these interventions are acceptable and have the potential to reduce STI rates. We will use our models to provide a quantitative assessment of the possible impact that this study suggests, so as to quantify the reduction of STI-incidence that dating apps' prevention campaigns [15].

In summary, the three objectives of the present study are to assess the percentage increase in STI cases resulting from dating apps, estimate the percentage of infected individuals who seek treatment, and appraise the positive impact of dating apps' pop-up ads may have in reducing STI incidence. These results are meritorious as they provide a quantitative assessments that can be used to inform public health initiatives.

2 A simple two-sex SIS model

We consider the sexually active population of the United States of two sexes that we will call *female* amd *male*, which we will identify with individuals aged 15 and above who have engaged in sexual contact (oral, vaginal, or anal).

STIs may be transmitted by all of these types of contact, through both same-sex and opposite-sex contacts.

Data concerning STI infections is quite detailed for the U.S. in the form of incidence (mostly) and prevalence (occasionally).

We shall use the definitions of *disease prevalence* and *disease incidence* from the CDC [7].

Definition 1: the number of cases of a disease (or infection) present at a given time is called *disease* (or *infection*) *prevalence* at that time.

Definition 2: the rate of new cases of a disease (or infection) appearing at a given time is called *disease* (or *infection*) *incidence* at that time.

We divide this population initially into four compartments, according to the two essential binary variables related to sexually transmitted infections, sex and infection status. Accordingly, our model has the following four compartments: STI-susceptible females, STI-infected females, STI-susceptible males, and STI-infected males. Later, we shall subdivide these four compartments into two disjoint compartments each, one of dating app users and another of non-users.

The size of the population at time t will be denoted $N = N(t)$, and the sizes of the four compartments will be denoted, respectively, as

$$S_f = S_f(t), \qquad I_f = I_f(t), \qquad S_m = S_m(t), \qquad I_m = I_m(t).$$

Because every individual is in exactly one of these compartments, it follows that

$$N = S_f + I_f + S_m + I_m. \tag{1}$$

We shall use the following notation $\big($with g representing sex, $g \in \{f, m\}\big)$:

$\xi_g =$ per capita exit rate from sexually active class of sex g for sex g by any reason > 0,

$\gamma_g =$ per capita recovery rate for sex g by successful treatment or by spontaneous recovery > 0,

$\Lambda_f =$ number of newly sexually active people who are female per unit time,

$\Lambda_m =$ number of newly sexually active people who are male per unit time,

$\lambda_g =$ per capita infection rate (*force of infection*) of sex-g susceptibles.

We consider same-sex and opposite-sex contacts, suggesting the following constitutive form for the forces of infection:

$$\lambda_f = C_{ff}\,\frac{I_f}{N} + C_{fm}\,\frac{I_m}{N}, \tag{2}$$

$$\lambda_m = C_{mm}\,\frac{I_m}{N} + C_{mf}\,\frac{I_f}{N}, \tag{3}$$

where, for $g_1, g_2 \in \{f, m\}$,

$$C_{g_1 g_2} = \text{ unit per capita probability of transmission from sex } g_2 \text{ to sex } g_1. \tag{4}$$

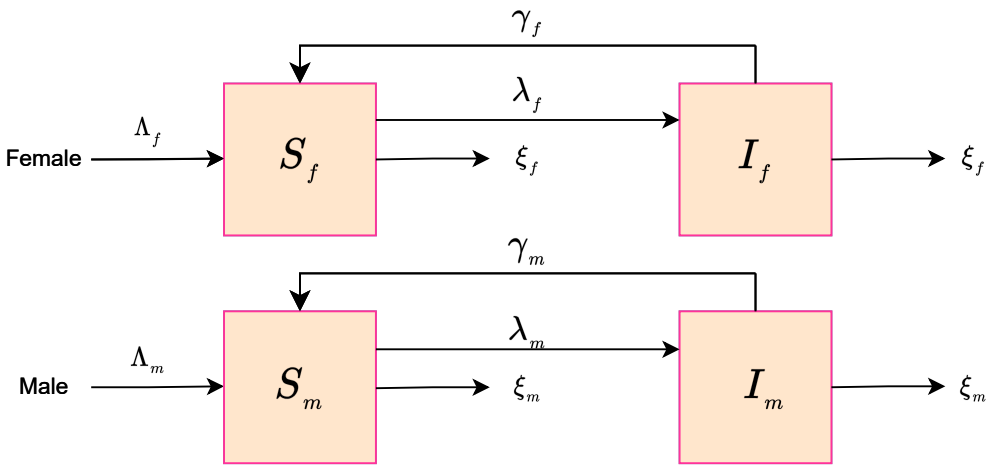

Figure 1: Flow diagram of the simple two-sex SIS model. Parameters over arrows are per capita rates, except for Λ and Λ_m which are total rates.

Our SIS model describing the evolution of the compartment sizes is the following:

$$\frac{d}{dt}S_f = \Lambda_f + \gamma_f I_f - \lambda_f S_f - \xi_f S_f S_f, \tag{5}$$

$$\frac{d}{dt}I_f = \lambda_f S_f - \gamma_f I_f - \xi_f I_f, \tag{6}$$

$$\frac{d}{dt}S_m = \Lambda_m + \gamma_m I_m - \lambda_m S_m - \xi_m S_m, \tag{7}$$

$$\frac{d}{dt}I_m = \lambda_m S_m - \gamma_m I_m - \xi_m I_m, \tag{8}$$

where, summing (5) with (6) and (7) with (8), we see that $F = S_f + I_f$ and $M = S_m + I_m$ satisfy the following ODEs:

$$\frac{dF}{dt} = \Lambda_f - \xi_f F, \tag{9}$$

$$\frac{dM}{dt} = \Lambda_m - \xi_m M. \tag{10}$$

respectively for the rates of sexual debut by females and males and for the per capita exit rates from the sexually active female and male populations, we see that the functions $F =$ number of sexually active females and $M =$ number of sexually active males have graphs shaped like learning curves, i.e. concave (convex if $F(0) > \Lambda_f/\xi_f$, respectively $M(0) > \Lambda_m/\xi_m$) functions that increase (decrease if convex) monotonically from their initial values $F(0)$ and $M(0)$ to their asymptotic values $F_\infty = \Lambda_f/\xi_f$ and $M_\infty = \Lambda_m/\xi_m$, respectively. Specifically,

$$F(t) = F(0)e^{-\xi_f t} + \frac{\Lambda_f}{\xi_f}(1 - e^{-\xi_f t}), \tag{11}$$

$$M(t) = M(0)e^{-\xi_m t} + \frac{\Lambda_m}{\xi_m}(1 - e^{-\xi_m t}). \tag{12}$$

Moreover, (11) and (12) imply that F is bounded by $\max\{F(0), \frac{\Lambda_f}{\xi_f}\}$ and M is bounded by $\max\{M(0), \frac{\Lambda_m}{\xi_m}\}$. Similarly, summing (11) and (12), we obtain the following ODE for the total population N:

$$\frac{dN}{dt} = \Lambda - \xi(t)N, \quad \text{with solution} \quad N(t) = F(0)e^{-\xi_f t} + \frac{\Lambda_f}{\xi_f}(1 - e^{-\xi_f t}) + M(0)e^{-\xi_m t} + \frac{\Lambda_m}{\xi_m}(1 - e^{-\xi_m t}),$$

where $\xi(t) = \xi_f \frac{F}{N} + \xi_m \frac{M}{N}$ is the (non-constant) per capita exit rate from the sexually active population at time t. However, for consistency, we prefer to have ξ constant and model N as solution of the learning curve model

$$\frac{dN}{dt} = \Lambda - \xi N, \quad \text{with solution} \quad N(t) = N(0)e^{-\xi t} + \frac{\Lambda}{\xi}(1 - e^{-\xi t}), \tag{13}$$

We point out that N is defined for all $t \geq 0$, is bounded above, and bounded away from 0. Therefore, the existence and uniqueness theorem for systems of ODEs guarantees the existence of a global unique solution to system (5)–(8) for any initial conditions.

For the systems representing only one of the sexes, (5)-(6) for females and (7)-(8) for males, we have the basic reproduction numbers

$$\mathcal{R}_0^f = \frac{C_{ff}\Lambda_f}{\bar{N}(\xi_f + \gamma_f)\xi_f} \qquad \text{and} \qquad \mathcal{R}_0^m = \frac{C_{mm}\Lambda_m}{\bar{N}(\xi_m + \gamma_m)\xi_m}. \tag{14}$$

Omitting the subindex that indicates the sex of the person when we consider only transmission within the same sex (making $\bar{N} = \Lambda/\xi$ and $\mathcal{R}_0 = C/(\xi + \gamma)$), we have for the system (5)-(6) or (7)-(8), a disease-free equilibrium

$$(S^*,\, I^*) = \left(\frac{\Lambda}{\xi}, 0\right)$$

and a unique endemic one that lies in the positive quadrant if, and only if, $\mathcal{R}_0 > 1$,

$$(\bar{S}, \bar{I}) = \left(\frac{(\xi + \gamma)\Lambda}{c\xi}, \frac{\Lambda}{\xi}\left(1 - \frac{\xi + \gamma}{c}\right)\right) = \left(\frac{\Lambda}{c\mathcal{R}_0}, \frac{\Lambda}{\xi}\left(1 - \frac{1}{\mathcal{R}_0}\right)\right).$$

We have the following stability results.

Theorem 1: [24] The disease-free equilibrium of the single-sex model (5)-(6) or (7)-(8) is globally asymptotically stable if $\mathcal{R}_0 \leq 1$ and unstable if $\mathcal{R}_0 > 1$. In the latter case, the endemic equilibrium is globally asymptotically stable.

3 Analysis of the Simple Two-Sex SIS Model

We will prove that solutions that begin non-negative, stay non-negative for all time.

Theorem 2: The non-negative orthant of $\mathbb{R}^4$ is invariant under the flow of system (5)–(8).

Proof: We first discard the trivial cases that have no infected individuals initially (i.e. $I_f(0) = I_m(0) = 0$). In that case, by uniqueness of solutions, the susceptible class of each sex evolves demographically according to the learning curve equations (11) and (12), while the infected classes are empty at all times.

We then assume that at least one the infected classes is initially non-empty, without loss of generality let

$$I_f(0) > 0. \tag{15}$$

It follows from (2) that $\lambda_f(0), \lambda_m(0) > 0$ and, by continuity, there is $\tilde{t} > 0$ such that

$$\lambda_f(t), \lambda_m(t) > 0, \qquad \text{for all } t \in [0.\tilde{t}). \tag{16}$$

Note that (5) and (7) imply that, for $t \in (0, \tilde{t})$ and $g = f, m$,

$$\frac{d}{dt}\left(S_g\, e^{\xi_g t + \int_0^t \lambda_g(\tau)d\tau}\right) = \left[\Lambda_g + \gamma_g I_g(t)\right] e^{\xi_g t + \int_0^t \lambda_g(\tau)d\tau} > 0, \tag{17}$$

whereby

$$S_g(t)\, e^{\xi_g t+\int_0^t \lambda_g(\tau)d\tau} - S_g(0) = \Lambda_g \int_0^t e^{\xi_g v+\int_0^v \lambda_g(\tau)d\tau} dv + \gamma_g \int_0^t I_g(v)\, e^{\xi_g v+\int_0^v \lambda_g(\tau)d\tau} dv > 0.$$

Hence, for all $t \in (0, \tilde{t})$ and $g = f, m$,

$$S_g(t) = S_g(0)\, e^{-\xi_g t-\int_0^t \lambda_g(\tau)d\tau} + \int_0^t \big[\Lambda_g + \gamma_g I_g(v)\big] e^{-\xi_g (t-v)-\int_v^t \lambda_g(\tau)d\tau} dv > 0. \tag{18}$$

Similarly, starting from (6) and (8) and writing the analogue of (17) for them, we can prove that for all $t \in (0, \tilde{t})$ and $g = f, m$,

$$I_g(t) = I_g(0)\, e^{-(\xi_g+\gamma_g)t} + \int_0^t e^{-(\xi_g+\gamma_g)(t-\tau)} \lambda_g(\tau) S_g(\tau) d\tau > 0. \tag{19}$$

Then, collecting (16), (18), and (19), for $t \in (0, \tilde{t})$ we have

$$S_f(t), I_f(t), S_m(t), I_m(t), \lambda_f, \lambda_m > 0. \tag{20}$$

We need to prove that the sizes of the four compartments stay positive for all time. Suppose they do not, and let t^* be the first positive time at which one of the four becomes empty: ($t^* \geq \tilde{t}$ by (20))

$$t^* = \inf\{t > 0 : S_f(t) \cdot S_m(t) \cdot I_f(t) \cdot I_m(t) = 0\}. \tag{21}$$

Note that (21) implies

$$S_f(t), I_f(t), S_m(t), I_m(t), \lambda_f(t), \lambda_m(t) > 0 \ \text{ for all } \ t \in (0, t^*). \tag{22}$$

Combining (18), (19), and (22), we see that

$$S_f(t^*), I_f(t^*), S_m(t^*), I_m(t^*), \lambda_f(t^*), \lambda_m(t^*) > 0$$

This contradicts the assumption on t^*, establishing that the solutions cannot vanish, thus concluding the proof.

□

We will prove next a classical threshold condition for the stability of the disease-free equilibrium [10]. Note that (5)–(8) readily yield an explicit expression for it: setting $\xi = \frac{\xi_f \xi_m}{X\xi_m + (1-X)\xi_f}$,

$$E_0 = \left(\frac{\Lambda_f}{\xi_f},\ 0,\ \frac{\Lambda_m}{\xi_m},\ 0\right), \text{ with total population } \bar{N} = \frac{\Lambda_f}{\xi_f} + \frac{\Lambda_m}{\xi_m} = \frac{\Lambda}{\xi}. \tag{23}$$

We compute next the basic reproduction number $\mathcal{R}_0$ as the spectral radius of the next generation matrix

$$G = \frac{1}{\bar{N}} \begin{pmatrix} \frac{C_{ff}}{\xi_f} \frac{\Lambda_f}{\xi_f+\gamma_f} & \frac{C_{fm}}{\xi_f} \frac{\Lambda_f}{\xi_m+\gamma_m} \\ \frac{C_{mf}}{\xi_m} \frac{\Lambda_m}{\xi_f+\gamma_f} & \frac{C_{mm}}{\xi_m} \frac{\Lambda_m}{\xi_m+\gamma_m} \end{pmatrix} = \begin{pmatrix} a & b \\ c & d \end{pmatrix}, \quad \text{where } \ a = \mathcal{R}_0^f,\ b = \frac{C_{fm}}{C_{ff}} \mathcal{R}_0^f,\ c = \frac{C_{mf}}{C_{mm}} \mathcal{R}_0^m,\ d = \mathcal{R}_0^m.$$

Because the off-diagonal coefficients of G have the same sign (they are both non-negative), G has two real non-negative eigenvalues,

$$0 \leq \frac{a+d}{2} - \frac{\sqrt{(a+d)^2 - 4(ad-bc)}}{2} \leq \frac{a+d}{2} + \frac{\sqrt{(a+d)^2 - 4(ad-bc)}}{2}.$$

Indeed, this follows because the discriminant $(\mathrm{tr}(G))^2 - 4\det(G) = (a-d)^2 + 4bc \geq 0$. Therefore,

$$\mathcal{R}_0 = \frac{\mathrm{tr}(G)}{2} + \sqrt{\frac{\mathrm{tr}^2(G)}{4} - \det(G)} = \frac{\mathcal{R}_0^f + \mathcal{R}_0^m}{2} + \sqrt{\frac{\mathrm{tr}^2(G)}{4} - \det(G)}. \tag{24}$$

Theorem 3: (see [10]) The equilibrium E_0 is locally asymptotically stable if $\mathcal{R}_0 < 1$ and unstable if $\mathcal{R}_0 > 1$.

Proof: First, note that the threshold condition $\mathcal{R}_0 < 1$ is equivalent to

$$\mathrm{tr}^2(G) - 4\det(G) < (2 - \mathrm{tr}(G))^2,$$

that is,

$$\boxed{\mathcal{R}_0 < 1 \iff 1 - \mathrm{tr}(G) + \det(G) > 0}. \tag{25}$$

We compute now the Jacobian matrix of the system (5)-(8) at E_0:

$$J(E_0) = \begin{pmatrix} -\xi_f & \gamma_f - \frac{C_{ff}}{N}\frac{\Lambda_f}{\xi_f} & 0 & -\frac{C_{fm}}{N}\frac{\Lambda_f}{\xi_f} \\ 0 & \frac{C_{ff}}{N}\frac{\Lambda_f}{\xi_f} - \xi_f - \gamma_f & 0 & -\frac{C_{fm}}{N}\frac{\Lambda_f}{\xi_f} \\ 0 & -\frac{C_{mf}}{N}\frac{\Lambda_m}{\xi_m} & -\xi_m & \gamma_m - \frac{C_{mm}}{N}\frac{\Lambda_m}{\xi_m} \\ 0 & \frac{C_{mf}}{N}\frac{\Lambda_m}{\xi_m} & 0 & \frac{C_{mm}}{N}\frac{\Lambda_m}{\xi_m} - \xi_m - \gamma_m \end{pmatrix}.$$

Its eigenvalues are the two negative real numbers,

$$-\xi_f, \quad -\xi_m,$$

and the two eigenvalues of the matrix

$$A = \begin{pmatrix} \frac{C_{ff}}{N}\frac{\Lambda_f}{\xi_f} - \xi_f - \gamma_f & \frac{C_{fm}}{N}\frac{\Lambda_f}{\xi_f} \\ \frac{C_{mf}}{N}\frac{\Lambda_m}{\xi_m} & \frac{C_{mm}}{N}\frac{\Lambda_m}{\xi_m} - \xi_m - \gamma_m \end{pmatrix}$$

A necessary and sufficient condition for them to have negative real part is that

$$\mathrm{tr}(A) < 0 \quad \text{and} \quad \det(A) > 0. \tag{26}$$

Note that, in view of (25), the condition $\mathcal{R}_0 < 1$ implies that

$$\frac{\mathcal{R}_0^f + \mathcal{R}_0^m}{2} < 1,$$

and so

$$(\mathcal{R}_0^f - 1) + (\mathcal{R}_0^m - 1) < 0.$$

The first condition in (26) is

$$(a-1)(\xi_f + \gamma_f) + (d-1)(\xi_m + \gamma_m) < 0.$$

The second condition in (26) is equivalent to

$$(a-1)(d-1) - bc = \det(G) - \mathrm{tr}(G) + 1 > 0,$$

which, by (25), is equivalent to $\mathcal{R}_0 < 1$. This proves the stability part of the theorem. The instability follows immediately from

$$\boxed{\mathcal{R}_0 > 1 \iff 1 - \mathrm{tr}(G) + \det(G) < 0 \iff \det(A) < 0}. \tag{27}$$

□

4 Parameter fitting for the simple SIS model

4.1 Initial Conditions

In order to run the model, ten parameters and four initial conditions need to be specified. We use the year 2009 as the initial one (corresponding to $t = 0$) so that we may compare model output with data for ten consecutive pre-pandemic years, 2010-2019. The years 2020 and 2021 were anomalous in terms of social and sexual contacts, and data for them should not be expected to fit well with output of autonomous dynamical systems such as those we use.

It is important to note that Definition 1 tells us the infection prevalence at a given time t is precisely the value of state variable $I(t)$, frequently reported as the proportion (percent) $I(t)/N(t)$. Similarly, Definition 2, when examined in view of (6) and (8), tells us that the infection incidence is precisely the value of $\lambda(t)S(t)$ = the acquisition rate of new infections at time t.

The initial conditions used for the number of susceptible and infected individuals of each sex are based on prevalence data derived from the National Health and Nutrition Examination Survey (NHANES) [list articles here/citation]. The data from NHANES is based from 2007-2012, and was used as an approximation for 2009 data, which is not available. For each age group this was calculated by multiplying the corresponding prevalence percentages by the corresponding population data from 2009. Females and males were separated by multiplying the prevalence population number by the proportion of the newly sexually active population that is female and by the proportion that is male. These were used as initial values for infected females and males in 2009, while the sizes of the susceptible compartments were calculated subtracting the initial numbers of infected from the total sexually active population of the corresponding sex.

4.2 Estimation of demographic parameters: Λ_g, and ξ_g

Of the ten model parameters, four can be obtained from demographic and other published data, namely

Λ_f = number of newly sexually active people who are female per unit time

Λ_m = number of newly sexually active people who are male per unit time, and

ξ_f and ξ_m, whose reciprocals are the median durations of the sexual lives for sex $g = f, m$.

Because our population of interest consists only of sexually active individuals, for whom data concerning the population sizes by sez is unavailable, we began by using data from the literature to build approximate sexually active population sizes by sex for the years 2009-2019.

We began by gathering data on the proportion of sexually active individuals by age and sex. Tables 3, 4, and 5 show the approximate percentages of sexually active and newly sexually active people in the U.S by age and sex.

The percentages of sexually active females and males of the given ages in table 3 are pulled from [1] for ages 15–20 (2011–2015 data), from a 2014 study on 'late in life virginity' [13] for ages 21–29, from [14] for ages 30–39 (2006–2008 data), and from [8] for ages 40-44 (2006–2008 data). We assume that people aged 45 or above who have never had sex will not debut sexually. We also assume that percentages for ages over 20 did not change during the period from 2010 to 2019 because there is no data available other than that we already used. The percentages in table 5 for ages 15-20 are pulled from a 2020 NCHS data brief on sexual activity and contraceptive use among teenagers [19] that used data from 2015 to 2017. Therefore, we updated for those ages the corresponding entries while keeping those for ages over 20 unchanged. Table 4 percentages of sexually active by sex and age are averages of those in Tables 3 and 5 to account for the fact that both [1] and [19] report data for 15- to 20-year-old people, respectively, for years 2011–2015 and 2015–2017.

age	% active females	% active males	% female debutantes	% male debutantes
15	11	16	11	16
16	25	27	14	11
17	42	41	17	14
18	55	55	13	14
19	69	68	14	13
20	75	75	6	7
21-24	87.7	85.7	12.7	10.7
25-29	95.2	95.6	7.5	9.9
30-34	97.6	96.7	2.4	0.1
35-39	98.5	98.4	0.9	2.7
40-44	99.6	98.7	1.1	0.3
45+	99.6	98.7	0	0

Table 3: Percentage by sex and age of sexually active U.S. population 2010-2014

The percentages of *newly* sexually active (debutantes) by age and sex were computed as differences of percentages of the sexually active population percentages from Tables 3, 4, and 5. Those percentages

age	% active females	% active males	% female debutantes	% male debutantes
15	16	18	16	18
16	31	30.5	15	12.5
17	47.5	44.5	16.5	14
18	60	58.8	12.5	14
19	71.5	69	11.5	10.5
20	77	76	5.5	7
21-24	87.7	85.7	12.7	10.7
25-29	95.2	95.6	7.5	9.9
30-34	97.6	96.7	2.4	0.1
35-39	98.5	98.4	0.9	2.7
40-44	99.6	98.7	1.1	0.3
45+	99.6	98.7	0	0

Table 4: Percentage by sex and age of sexually active U.S. population 2015

age	% active females	% active males	% female debutantes	% male debutantes
15	21	20	21	20
16	37	34	16	14
17	53	48	16	14
18	65	62	12	14
19	74	70	9	8
20	79	77	5	7
21-24	87.7	85.7	8.7	8.7
25-29	95.2	95.6	7.5	9.9
30-34	97.6	96.7	1.4	1.1
35-39	98.5	98.4	0.9	1.7
40-44	99.6	98.7	1.1	0.3
45+	99.6	98.7	0	0

Table 5: Percentage by sex and age of sexually active U.S. population 2016-2019

were then multiplied by the size of the corresponding age and sex group for each year desired (available from the National Bureau of Census and Statistics). Summing over all age groups for each sex provided us with the total number of newly sexually active females and males for each year from 2009 to 2019.

The sexually active population sizes by sex were used to fit the three parameters of each of the single-sex learning curve models (11) and (12), and those for the total sexually active population (13).

Figure 2 shows the fitting by our learning curve model (11) of the size of the U.S. female sexually active population for the years 2009-2019 calculated from demographic data as explained above, as well as that data. We fitted the three constants $F_0 = F(0)$, Λ_f, and ξ_f to the population data and obtained an excellent fit (maximum annual deviation approximately 0.6%) with the values

$$F_0 = 114,425,275, \qquad \Lambda_f = 3,630,878, \qquad \xi_f = 0.021085. \tag{28}$$

Similarly, we show in Figure 3 the fitting of and the size of the U.S. male sexually active population for the same years. The three constants fitted were $M_0 = M(0)$, Λ_m, and ξ_m and we obtained again an excellent fit (maximum annual deviation less than 0.5%) with the values

$$M_0 = 106,724,822, \qquad \Lambda_m = 3,768,331, \qquad \xi_m = 0.025003. \tag{29}$$

We also fitted the parameters of eqN to the sizes of the total U.S. sexually active population for the years 2009-2019. The three constants fitted this time were $N_0 = N(0)$, Λ, and ξ and the fit obtained was just as good (maximum annual deviation approximately 0.5%), with the values

$$N_0 = 221,150,097, \qquad \Lambda = 7,399,209, \qquad \xi = 0.023069. \tag{30}$$

We now have determined the following four parameters for our 4-compartment SIS model,

$$X = \frac{\Lambda_f}{\Lambda} \ \text{(from (28) and (30))}, \quad \Lambda \ \text{(from (30))}, \quad \xi_f \text{ and } \xi_m \ \text{(from (28) and (29))}.$$

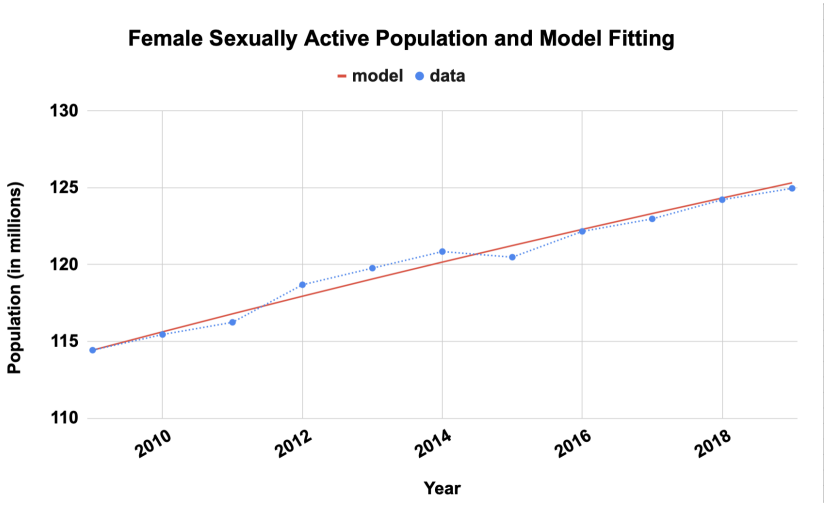

Figure 2: Learning curve fitting of female sexually active population, $F(t) = F(0)e^{-\xi_f t} + \frac{\Lambda_f}{\xi_f}(1 - e^{-\xi_f t})$.

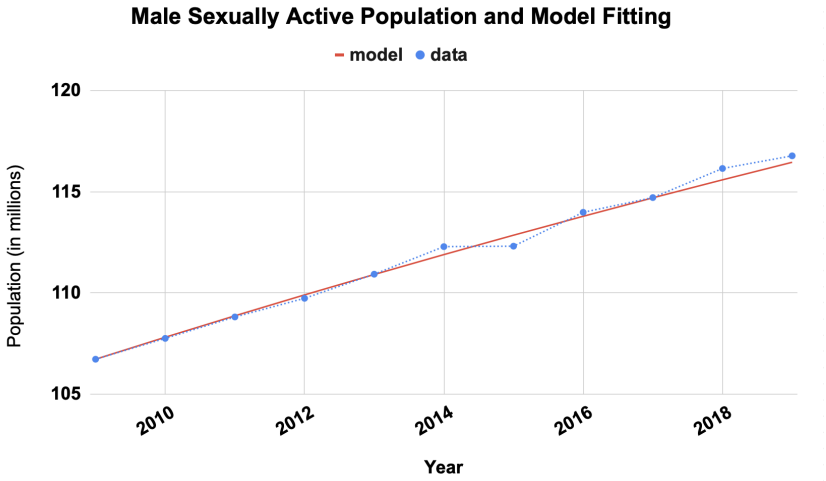

Figure 3: Learning curve fitting of male sexually active population, $M(t) = M(0)e^{-\xi_m t} + \frac{\Lambda_m}{\xi_m}(1 - e^{-\xi_m t})$.

4.3 Estimation of epidemiological parameters: γ_g and $C_{g_1 g_2}$

Concerning the eight-compartment model, there were six fitted parameters, 4 fixed parameters, and 4 fitted parameters. The 4 initial and 4 fixed parameters are S_f, S_m, I_f, and I_m and λ_f, λ_m, ξ_m, and ξ_f, respectively. These were found using the methods detailed in section 4.1 and 4.2. The fitted parameters were obtained using the method detailed below.

Note that each of the *effective unit contact rates* $C_{g_1 g_2}$ in (4) is a product of a behavioral parameter and an epidemiological one,

$$C_{g_1 g_2} = \eta_{g_1 g_2}\, \rho_{g_1 g_2},$$

where

$$\rho_{g_1 g_2} = \text{ expected number (median) of sexual contacts per unit time of a person of sex } g_2 \text{ with persons of sex } g_1,$$

and

$$\eta_{g_1 g} = \text{ probability of an infected person of sex } g_2 \text{ transmitting infection to a susceptible (uninfected) person of sex } g_1 \text{ during a sexual contact (}\textit{transmissibility}\text{).}$$

The factors making up each of the parameters $C_{g_1g_2}$ do not appear separately in our model, but rather only as their product; therefore, we do not need to identify them separately. The effective unit contact rates themselves will be identified by parameter fitting to incidence data.

The parameters $\rho_{g_1g_2}$, however, can be estimated using data for sexual identity-behavior [11]. Sexual identity in that study was given as 100% heterosexual, mostly straight/bisexual, or mostly gay/100% gay, while sexual behavior was defined as opposite sex only or both-sexes sex. The data for females aged 24-32 is given in Table 3 and for males aged 24-32 in Table 4. This data is compiled from answers to the questions "Considering all types of sexual activity, with how many male partners have you ever had sex?" and "Considering all types of sexual activity, with how many female partners have you ever had sex?"

		100% Heterosexual		Mostly Straight/Bisexual		Mostly Gay/100% Gay
	total sample	op. sex only	both sex sex	op. sex only	both sex sex	both sex sex
Respondents (N)	7392	5607	307	716	629	133
STI Rate	46.63	43.62	58.09	51.11	64.19	32
Sexual Partners (N)	10.41	7.7	15.84	11.63	27.7	16.5

Table 6: Females (24-32) Sexual Identity-Behavior

		100% Heterosexual		Mostly Straight/Bisexual		Mostly Gay/100% Gay	
	total sample	op. sex only	both sex sex	op. sex only	both sex sex	same sex only	both sex sex
Respondents (N)	6323	5744	151	142	117	94	75
STI Rate	32.67	31.96	41.36	32.04	43.66	39.41	48.85
Sexual Partners (N)	17.64	17.1	20.21	12.09	26.92	37.45	29.47

Table 7: Males (24-32) Sexual Identity-Behavior

The mean age for women is 28.7 and 28.9 for men. The median age of sexual debut is 17.2 for females and 16.8 for males [5]. We may estimate the average time since sexual debut for females in the study as $28.7 - 17.2 = 11.5$, and for males as $28.9 - 16.8 = 12.1$.

We compute now the median numbers of sexual partners that sexually active women have per year, of the opposite sex, a_f —as the weighted average of the numbers of partners reported in columns 3 and 5 of Table 3— and of the same sex, b_f —as the weighted average of the numbers of partners reported in columns 4, 6, and 7 of Table 3:

$$a_f = \left(\frac{5607}{5607+716}\right)\cdot(7.7) + \left(\frac{716}{5607+716}\right)\cdot(11.63) \approx 8.15.$$

$$b_f = (\frac{307}{307+629+133})\cdot(15.84) + (\frac{629}{307+629+133})\cdot(27.7) + (\frac{133}{307+629+133})\cdot(16.5) \approx 22.9.$$

Finally, we compute the annual numbers as ratios.

$$\rho_{fm} = \frac{8.15}{11.5} \approx 0.709, \qquad \rho_{ff} = \frac{22.9}{11.5} \approx 1.99. \tag{31}$$

Similarly, we compute the median numbers of sexual partners that sexually active men have per year, of the opposite sex, a_m —as the weighted average of the numbers of partners reported in columns 3 and 5 of Table 4— and of the same sex, b_m —as the weighted average of the numbers of partners reported in columns 4, 6, 7, and 8 of Table 4:

$$a_m = \left(\frac{5744}{5744+142}\right)\cdot(17.1) + \left(\frac{142}{5744+142}\right)\cdot(12.09) \approx 17.0$$

$$b_m = \frac{1}{437}\big[(151)\cdot(20.21) + (117)\cdot(26.92) + (94)\cdot(37.45) + (75)\cdot(29.47)\big] \approx 27.3.$$

Now, we may compute the annual numbers for men as ratios.

$$\rho_{mf} = \frac{17.0}{12.1} \approx 1.40, \qquad \rho_{mm} = \frac{27.3}{12.1} \approx 2.26. \tag{32}$$

The *sexual preference* parameters, ν_g, are the fractions of all sexual contacts of persons of sex g that are with persons of the opposite sex (that can separate same-sex contacts from opposite-sex contacts):

$$\nu_f = \frac{a_f \cdot 6323}{a_f \cdot 6323 + b_f \cdot 1069} \approx 67.8\%, \qquad \nu_m = \frac{a_m \cdot 5886}{a_m \cdot 5886 + b_m \cdot 437} \approx 89.3\%. \tag{33}$$

Concerning the parameters $\eta_{g_1 g_2}$, there is some scattered information for the three STIs of our study, for example, [2] reports chlamydial $\eta_{g_1 g_2} = 0.022 - 0.044$ for the four types of sexual partnerships combined. On the other hand, [16] reports some probabilities of transmission per type of sex act for gonorrhea that can be combined as: $\eta_{fm} = 0.5 - 0.84$, $\eta_{mf} = 0.02 - 0.2$, and $\eta_{mm} = 0.63 - 0.84$. We see wide ranges of values and disparate orders of magnitude for different STIs have been reported. Therefore, we decided to identify the transmissibilities for our model (together with the per capita recovery rates) by fitting them to incidence data. Still, for reference purposes, we compute them from the ρ and η values above:

$$C_{ff} \approx 1.99(0.033) = 0.00657, \qquad C_{fm} \approx 0.709(0.6) = 0.0395, \tag{34}$$

$$C_{mf} \approx 1.40(0.05) = 0.07, \qquad C_{mm} \approx 2.26(0.7) = 1.58. \tag{35}$$

The parameters representing unit effective contact rates and per capita recovery rates of our model (5)–(8) are fitted to available annual data of incidence by sex of gonorrhea. We fitted five years of incidence data (2014-2019, with 10 data points in total). The fitting of the model to incidence data was performed in the software MATLAB, using the routine "lsqcurvefit" which determined the parameter values $(\gamma_f, \gamma_m, C_{ff}, C_{fm}, C_{mm}, C_{mf})$ that minimize the sum of the squared deviations. The results of the parameter fitting are shown in Figure 4, and the estimated parameter values are presented in Table 8.

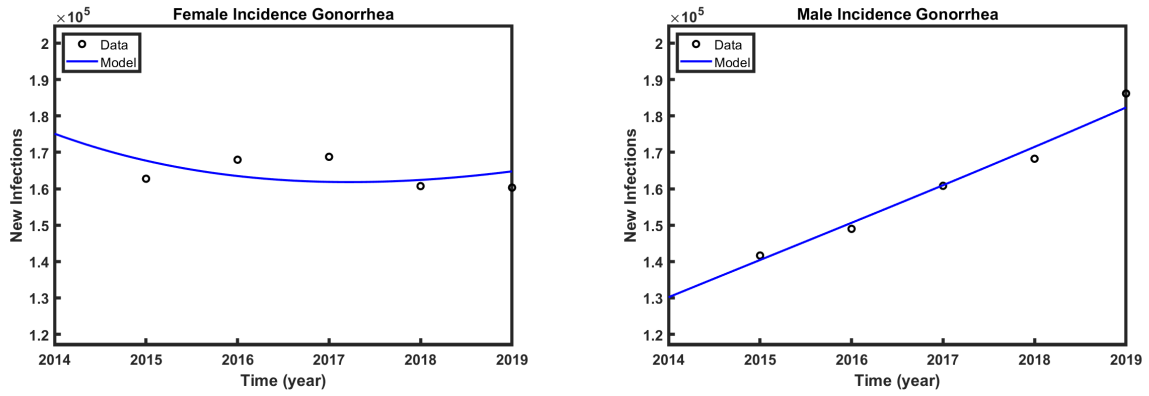

(a) (b)

Figure 4: Fitting of the simple model to incidence data.

Parameter	Fitted Value	Parameter	Fitted Value
$S_f(0)$	123,388,000	$S_m(0)$	115,731,000
$I_f(0)$	35,000	$I_m(0)$	990,000
Λ_f	3,876,624	Λ_m	3,887,378
ξ_f	0.021	ξ_m	0.025
γ_f	0.100	γ_m	0.185
C_{ff}	0.050	C_{mm}	0.265
C_{fm}	0.343	C_{mf}	0.245

Table 8: Initial, fixed, and fitted parameters of the simple model to incidence data.

The reciprocals of the parameters μ_g represent the median (expected value) of the remaining life of people of sex g in the sexually active population (i.e. *life expectancy* at age 15). These can be obtained from life tables [3], $1/\mu_f = 66.8$ and $1/\mu_g = 62.1$. Thus,

$$\mu_f = 0.0150, \qquad \mu_m = 0.0161. \tag{36}$$

The reciprocals of the parameters ξ_g represent the median (expected value) of the permanence of people of sex g in the sexually active population (*length of sexual life*). They are estimated later (by fitting to our sexually active population data, see (28) and (29)) to be $1/0.021085 \approx 47.4$ years for women and $1/0.025003 \approx 40.0$ for men. From them, we may obtain estimates for $\kappa_g = \xi_g - \mu_g$ (that are not really needed):

$$\kappa_f = 0.021085 - 0.0150 \approx 0.0061, \qquad \kappa_m = 0.025003 - 0.0161 \approx 0.0089. \tag{37}$$

The reciprocals of the parameters γ_g represent the median (expected value) of the duration of infection for infected people of sex g. Those may differ significantly because of the different courses that infection may follow for different individuals. Infected people may be symptomatic or asymptomatic. The former may or may not seek treatment, while the latter may or may not recover spontaneously. The asymptomatic who do not recover spontaneously may discover their infection through screening. Let us introduce seven parameters related to infection and recovery to quantify these different courses of infection,

$\zeta =$ percent of infections that are asymptomatic $= 0.7$, [18, 22]
$\theta =$ percent of identified (by symptoms or screening) infected who seek treatment,
$\sigma =$ percent of asymptomatic (infected or uninfected) that are screened,
$\varphi =$ percent of infections that clear spontaneously $=$ 0.22–0.74, [12]
$T_{\text{SC}} =$ median duration of spontaneous clearing $= 1.25$, [20]
$T_{\text{OT}} =$ median wait from diagnosis until treatment onset: 0–1/52, (estimated)
$T_{\text{T}} =$ median duration of treatment $= 1/52$. [6]

We can decompose the duration of infection for infected people of sex g as follows:

$$\begin{aligned}\frac{1}{\gamma_g} = \zeta\left[\varphi\cdot T_{\text{SC}} + (1-\varphi)\cdot\left(\sigma\cdot\theta\cdot\left(T_{\text{OT}}+T_{\text{T}}\right) + \left((1-\sigma)+\sigma\cdot(1-\theta)\right)\frac{1}{\xi_g}\right)\right] \\ + (1-\zeta)\left[(1-\theta)\cdot\left((1-\varphi)\cdot\frac{1}{\xi_g} + \varphi\cdot T_{\text{SC}}\right) + \theta\cdot\left(T_{\text{OT}}+T_{\text{T}}\right)\right].\end{aligned} \tag{38}$$

We estimated T_{SC} by fitting an exponential decay function at rate k to the data reported in [20], with an almost perfect fit to the values of still-infected cases after 1, 2, 3, and 4 years for $k = 0.8$. Its reciprocal is our estimate for $T_{\text{SC}} = 1.25$. We proceed now to use (38) to see how estimated parameter values fit together in this balance equation applied to data for females. We estimated $\gamma_f = 0.9745$ by fitting our model parameters to the combined incidence data for gonorrhea and chlamydia from 2010 to 2014. Because σ and θ are not found in the literature, we look in Figure 5 at the functional dependence of the former on the latter derived from (38) for the stated values of the remaining 7 parameters ($\varphi = 0.74$).

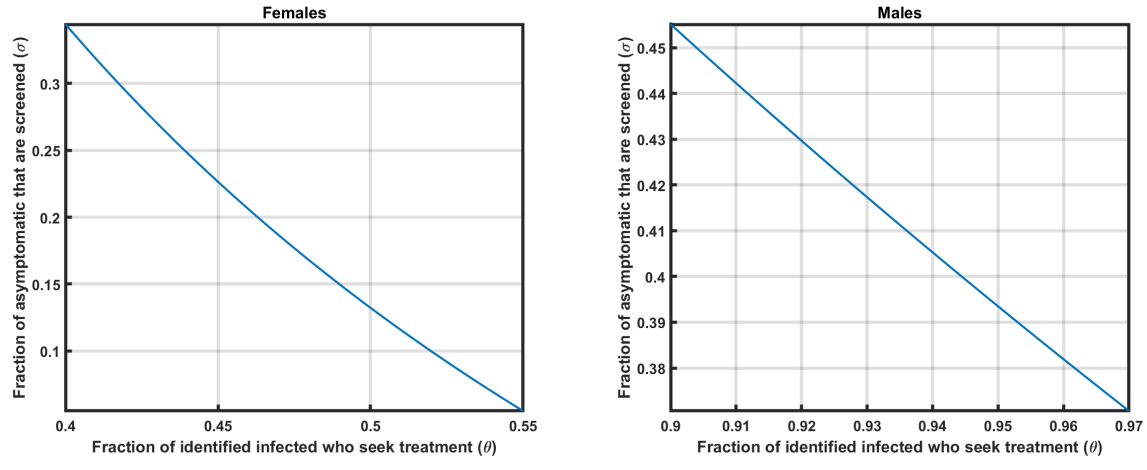

(a) (b)

Figure 5: Percentage screening as a function of percentage treatment-seekers

We see in Figure 5 that, when 90%–97% of detected infections in males are treated, there needs to be 37%–40.5% screening of non-symptomatic (susceptibles and infecteds), with the needed screening to balance the duration-of-infection equation (38) becoming larger as φ decreases, with no possible values for σ and θ as φ approaches the smallest value in its range, 0.22.

In summary, it is likely that the percentage of identified infections that are treated is very high, between 90% and 97%, because otherwise some of the other model parameters would have to take on values that do not seem realistic for the population and the STIs under study. (39)

5 An STI SIS model for dating app users

We now assign the individuals of each sex to compartments based on the two factors that are at the center of this study, namely dating application status (user vs. non-user) and infection status (susceptible vs. infected) for the two bacterial, most common, curable STIs (chlamydia and gonorrhea). Thus our model has the following eight compartments: susceptible female users of dating apps, infected female users of dating apps, susceptible male users of dating apps, infected male users of dating apps, susceptible female non-users of dating apps, infected female non-users of dating apps, susceptible male non-users of dating apps, infected male non-users of dating apps. The sizes of these compartments will be denoted, respectively, as

$$S_f^u = S_f^u(t), \qquad I_f^u = I_f^u(t), \qquad S_m^u = S_m^u(t), \qquad I_m^u = I_m^u(t), \tag{40}$$

$$S_f^{nu} = S_f^{nu}(t), \quad I_f^{nu} = I_f^{nu}(t), \quad S_m^{nu} = S_m^{nu}(t), \quad I_m^{nu} = I_m^{nu}(t). \tag{41}$$

Because every individual is in exactly one of these compartments, it follows that

$$N = S_f^u + I_f^u + S_m^u + I_m^u + S_f^{nu} + I_f^{nu} + S_m^{nu} + I_m^{nu}. \tag{42}$$

We shall keep the meaning of the parameters Λ_g, and ξ_g (because they are demographic, independent of app use and infection) and introduce the notation, for $s = n, u$,

$\Lambda_g^s =$ number of newly sexually active people entering compartment of sex g and app user status s,
$\gamma_g^s =$ per capita recovery rate in compartment of sex g and app user status s,
$\lambda_g^s =$ per capita infection rate (*force of infection*) in compartment of sex g and app user status s.

In this setting, unlike in our simple SIS model (5)–(8), we formally model opposite-sex contacts only. Same-sex contacts are not considered separately due to a lack of data of sexual partners by dating app usage, and also to avoid the need for an additional 8 constants (the effective same-sex contact rates by infection and by dating-app-use status. This may not affect our conclusions too much because, for individuals of each sex, the proportion of same-sex contacts is fairly small within all their sexual contacts.

Consequently, the constitutive form of the forces of infection are given by

$$\begin{aligned}
\lambda_f^n &= C_{fm}^{nn} I_m^n + C_{fm}^{nu} I_m^u, \\
\lambda_m^n &= C_{mf}^{nn} I_f^n + C_{mf}^{nu} I_f^u, \\
\lambda_f^u &= C_{fm}^{un} I_m^n + C_{fm}^{uu} I_m^u, \\
\lambda_m^u &= C_{mf}^{un} I_f^n + C_{mf}^{uu} I_f^u,
\end{aligned} \tag{43}$$

where, for $g_1, g_2 \in \{f, m\}$, $s_1, s_2 \in \{u, n\}$,

$$0 < C_{g_1 g_2}^{s_1 s_2} = \text{ unit per capita infectivity from sex } g_2 \text{ and status } s_2 \text{ to sex } g_1 \text{ and status } s_1. \tag{44}$$

Furthermore, we shall assume that the initial, non-negative compartment sizes satisfy the following equilibrium condition for the total recruitment and mortality rates:

$$\begin{aligned}
&N_0 = S_f^u(0) + I_f^u(0) + S_m^u(0) + I_m^u(0) + S_f^n(0) + I_f^n(0) + S_m^n(0) + I_m^n(0) = \Lambda/\mu, \text{ where} \\
&\Lambda = \Lambda_f^u + \Lambda_m^u + \Lambda_f^{nu} + \Lambda_m^n, \quad \text{and} \quad \textstyle\sum_{g,s} I_g^s(0) > 0 \text{ so that there is STI transmission.}
\end{aligned} \tag{45}$$

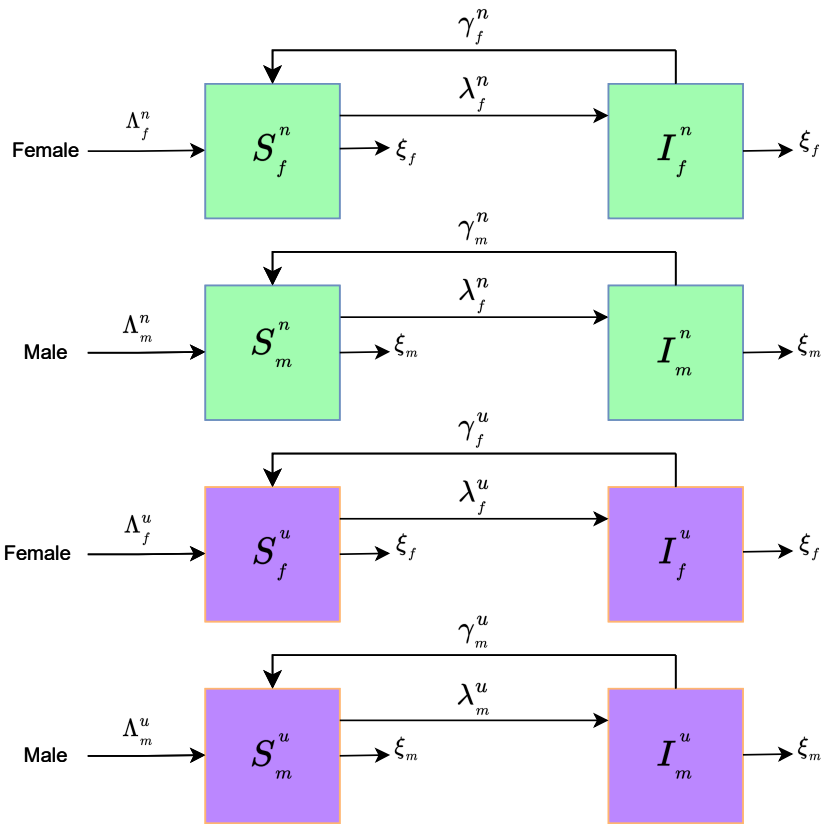

Figure 6: Flow diagram of our dating app STI model. The parameters over the arrows are per capita rates, except for inflow parameters into susceptible compartments that represent total rates.

Figure 6 shows the flow diagram for our dating app model, where the parameters over each arrow are per capita transition rates, with the exception of the inflow parameters into susceptible compartments that represent total rates.

Our dynamical system model describing the evolution of the compartment sizes is the following:

$$\frac{d}{dt}S_f^n = \Lambda_f^n + \gamma_f^n I_f^n - \lambda_f^n S_f^n - \xi_f S_f^n, \tag{46}$$

$$\frac{d}{dt}I_f^n = \lambda_f^n S_f^n - \xi_f I_f^n - \gamma_f^n I_f^n, \tag{47}$$

$$\frac{d}{dt}S_m^n = \Lambda_m^n + \gamma_m^n I_m^n - \lambda_m^n S_m^n - \xi_m S_m^n, \tag{48}$$

$$\frac{d}{dt}I_m^n = \lambda_m^n S_m^n - \xi_m I_m^n - \gamma_m^n I_m^n, \tag{49}$$

$$\frac{d}{dt}S_f^u = \Lambda_f^u + \gamma_f^u I_f^u - \lambda_f^u S_f^u - \xi_f S_f^u, \tag{50}$$

$$\frac{d}{dt}I_f^u = \lambda_f^u S_f^u - \xi_f I_f^u - \gamma_f^u I_f^u, \tag{51}$$

$$\frac{d}{dt}S_m^u = \Lambda_m^u + \gamma_m^u I_m^u - \lambda_m^u S_m^u - \xi_m S_m^u, \tag{52}$$

$$\frac{d}{dt}I_m^u = \lambda_m^u S_m^u - \xi_m I_m^u - \gamma_m^u I_m^u. \tag{53}$$

Note that summing equations (46)–(53), it follows from (1) that

$$\frac{dN}{dt} = \Lambda - \xi N. \tag{54}$$

Using the initial condition (45), we see that the total population N is constant,

$$N \equiv N_0. \tag{55}$$

6 Well-posedness of the dating app model

We need to show that the non-negative orthant of $\mathbb{R}^8$ is invariant under the flow of system (50)–(49). This is done in an entirely analogous way as for the simple model, Theorem 2.

Starting with the equations for the four compartments of susceptible individuals, equations (46), (48), (50), and (52), we write equivalent ones (which are just (17) with the parameters distinguishing now app-user status)

$$\frac{d}{dt}\left(S_g^s e^{\xi_g t+\int_0^t \lambda_g^s(\tau)d\tau}\right) = \left[\Lambda_g^s + \gamma_g^s I_g^s(t)\right] e^{\xi_g t+\int_0^t \lambda_g^s(\tau)d\tau} > 0, \qquad g \in \{f,m\}, \quad s \in \{n,u\},$$

whereby

$$S_g^s(t)e^{\xi_g t+\int_0^t \lambda_g^s(\tau)d\tau} - S_g^s(0) = \Lambda_g^s \int_0^t e^{\xi_g v+\int_0^v \lambda_g^s(\tau)d\tau}dv + \gamma_g^s \int_0^t I_g^s(v)\, e^{\xi_g v+\int_0^v \lambda_g^s(\tau)d\tau}dv.$$

Hence, for $g \in \{f,m\}$, $s \in \{n,u\}$, and as long as the infected class sizes stay positive,

$$S_g^s(t) = S_g^s(0)\, e^{-\xi_g t-\int_0^t \lambda_g^s(\tau)d\tau} + \int_0^t \left[\Lambda_g^s + \gamma_g^s I_g^s(v)\right] e^{-\xi_g (t-v)-\int_v^t \lambda_g^s(\tau)d\tau}dv > 0. \tag{56}$$

Concerning the four compartments of infected individuals, we note that (43)–(45) imply that at least one of the four compartments of infected is non-empty, say I_f^N; this makes the two forces of infection $\lambda_f^n > 0$ and $\lambda_f^u > 0$ whereby, by continuity of solutions, for $t > 0$ small enough, necessarily $I_f^n(t) > 0$, $I_m^n(t) > 0$, and $I_M^u(t) > 0$. Hence $\lambda_f^u(t) > 0$ for $t > 0$ small enough and, even if $\lambda_f^u(0) = 0$, (51) leads to $I_f^u(t) > 0$ for $t > 0$ small enough.

Also, equations (47), (49), (51), and (53) imply that, as long as the sizes of the susceptible classes are positive,

$$I_g^s(t) = I_g^s(0)\, e^{-\xi_g t-\int_0^t \lambda_g^s(\tau)d\tau} + \int_0^t \lambda_g^s(v)\, S_g^s(v)\, e^{-\xi_g (t-v)-\int_v^t \lambda_g^s(\tau)d\tau}dv > 0. \tag{57}$$

In summary, for $t > 0$ small enough, $S_g^s(t) > 0$ and $I_g^s(t) > 0$ for all four combinations of sex and dating-app-user status. We want to show that the positivity stays true *for all* time $t > 0$.

Suppose that this is not the case, and consider the smallest positive time $\bar{t}$ at which one of these eight compartments of susceptible or infected individuals is empty,

$$\bar{t} = \min\{t > 0 : S_f^n(t) \cdot S_f^u(t) \cdot S_m^n(t) \cdot S_m^u(t) \cdot I_f^n(t) \cdot I_f^u(t) \cdot I_m^n(t) \cdot I_m^u(t) = 0\}. \tag{58}$$

It follows that, for $t \in (0,\bar{t})$, $S_f^n(t), S_f^u(t), S_m^n(t), S_m^u(t) > 0$, $I_f^n(t), I_f^u(t), I_m^n(t), I_m^u(t) > 0$ and *a fortiori*, because of (43), we have all four forces of infection positive on that interval: $\lambda_f^n(t)$, $\lambda_f^u(t)$, $\lambda_m^n(t)$, $\lambda_m^u(t) > 0$ for $t \in (0,\bar{t})$. Consequently, because of (56) and (57), we have

$$S_f^n(\bar{t}), S_f^u(\bar{t}), S_m^n(\bar{t}), S_m^u(\bar{t}) > 0, I_f^n(\bar{t}), I_f^u(\bar{t}), I_m^n(\bar{t}), I_m^u(\bar{t}) > 0,$$

contradicting (58). Hence, such time does not exist and we have proved the following result.

Theorem 4: The non-negative orthant of $\mathbb{R}^8$ is invariant under the flow of system (46)–(53).

7 Parameter Fitting for the STI SIS model for dating app users

The 8-Compartment STI SIS model for dating app users, (46)–(53), involves 6 demographic parameters that were identified for the simple two-sex SIS model, namely $\Lambda_f^n, \Lambda_m^n, \Lambda_f^u, \Lambda_m^u, \xi_f$, and ξ_m. For that model we actually identified $\Lambda_f = \Lambda_f^n + \Lambda_f^u$ and $\Lambda_m = \Lambda_m^n + \Lambda_m^u$, which we separated into app-user and non-user based on the percentages of each of these statuses derived from data contained in [9].

The 8-Compartment STI SIS model for dating app users also contains 12 epidemiological parameters that need fitting to chlamydia/gonorrhea incidence data by sex. These parameters were estimated using MATLAB, specifically the routine "fminsearch" to minimize the maximum of the deviations between the model output and incidence data. The parameter names and their estimated value are shown in Table 9, while the graphs of the model output together with the incidence data appear in Figure 7.

Parameter	Fitted Value
γ_f^n	2.462
γ_f^u	0.307
γ_m^n	0.387
γ_m^u	1.338
C_{mf}^{nn}	4.624
C_{mf}^{un}	2.197
C_{mf}^{nu}	0.247
C_{mf}^{uu}	8.437
C_{fm}^{nn}	0.100
C_{fm}^{un}	0.100
C_{fm}^{nu}	3.794
C_{fm}^{uu}	2.968

Table 9: Parameters estimated by fitting the model to incidence data.

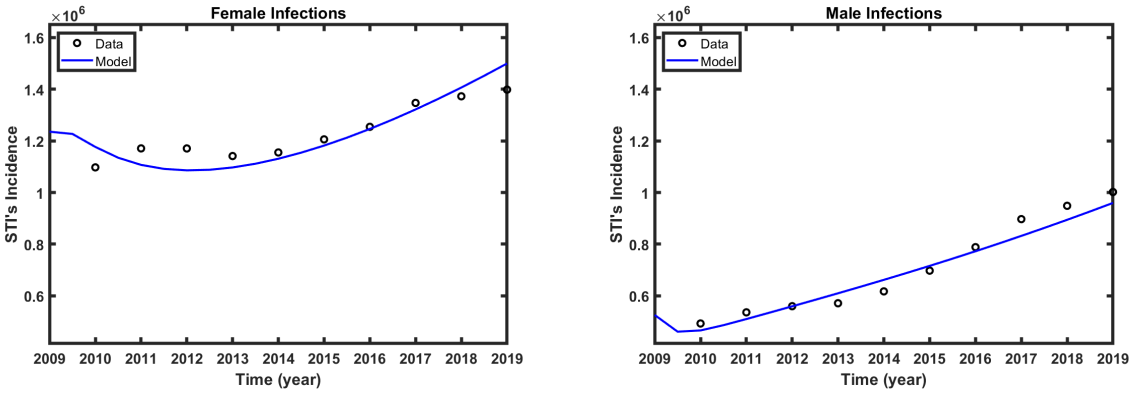

(a) (b)

Figure 7: Fitting of the STI SIS model for dating app users to incidence data.

8 Simulations

8.1 STI Incidence on the Rise

Figures 7-10 present the annual increase in male and female STI prevalence due to dating apps that has occurred between 2015 and 2019. As shown, the percent of change in STI prevalence has decreased as a function of increasing time for both males and females; however the percentage of change levels off at a positive value for both populations. As such, these figures indicate that research towards understanding the dynamics of STIs and dating apps is a worthwhile endeavor.
Regarding female prevalence, Figure 8 conveys that between 2018 and 2019 there was a 8.7% increase in female prevalence due to dating apps. Moreover, this percent increase is shown to stabilize at this value, indicating that STI prevalence is continuing to increase annually as a function of increasing time. In a similar fashion, Figure 9 presents a 9.2% increase in male prevalence due to dating apps between 2018 and 2019, with the annual percentage of change stabilizing at around 8-9% with increasing time.

Consistent with the trends discussed above, Figures 10 and 11 referring to the annual percentage of change in female and male incidence over time display their trend-lines stabilizing at 9.9% and 6% respectively. As all four figures indicate the stabilization of the annual percentage of change in STIs is a positive value, it is suggested that both the incidence and prevalence of STIs are continuing to rise over time. This information provides additional motivation for the inquiry into the quantifiable effects of dating app usage upon the proliferation of STIs.

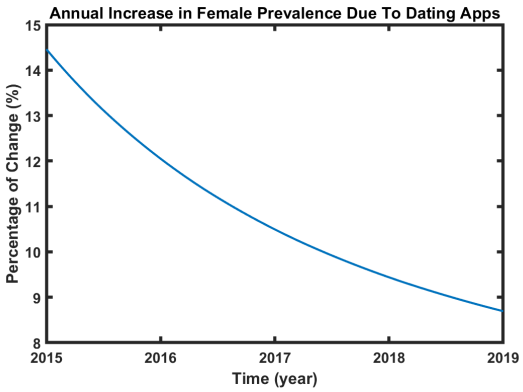

Figure 8: Female Prevalence

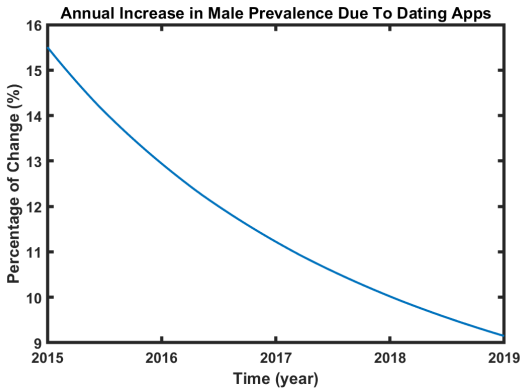

Figure 9: Male Prevalence

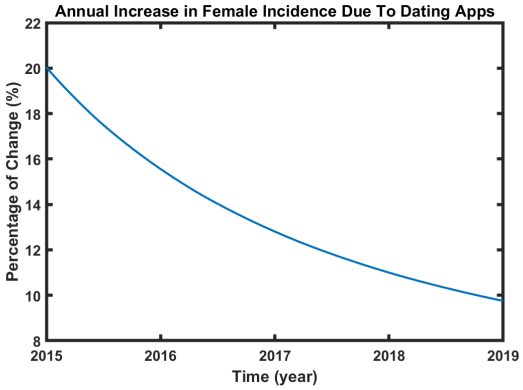

Figure 10: Female Incidence

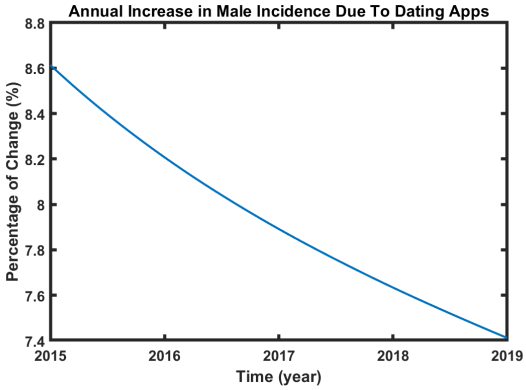

Figure 11: Male Incidence

8.2 Sensitivity Analysis

We performed sensitivity analyses of incidence and prevalence by sex for four γ_g^s parameters and eight $C_{g_1 g_2}^{s_1 s_2}$ parameters. We found that γ_m^u and γ_f^u have the greatest impact on the prevalence and incidence of the STIs in our study (chlamydia and gonorrhea), because the sensitivity indexes of incidence and prevalence with respect to these parameters were the largest in magnitude. This finding is consistent with the literature, as users of dating apps are shown to engage in more risky behavior that is linked to STI transmission. The corresponding sensitivity curves are shown below, where the baseline values correspond to the fitted ones shown in Table 9.

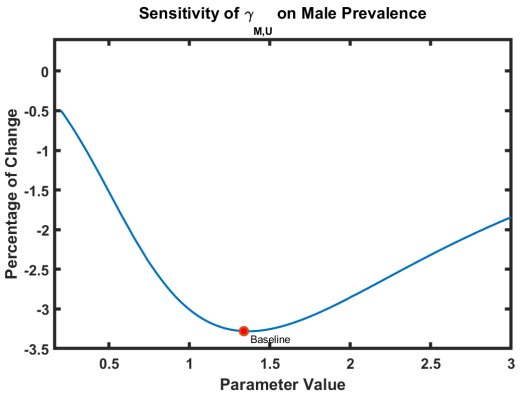

Figure 12: male prevalence γ_m^u

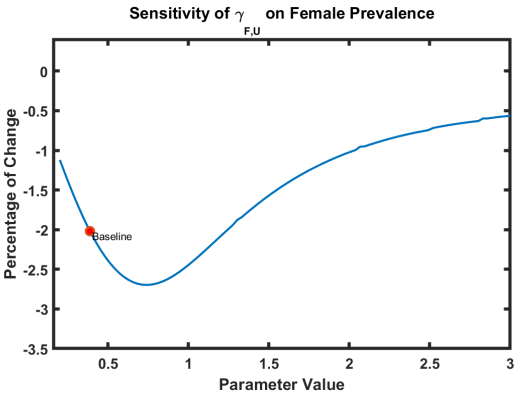

Figure 13: female prevalence γ_f^u

With regard to the sensitivity curve for $\gamma_{M,U}$, a 1% increase in the parameter value results in a 3.4% decrease in male prevalence and a 3.1% decrease in female prevalence. In contrast, based on Figure 5, a 1% increase in the $\gamma_{F,U}$ results in a 2.65% decrease in female prevalence and a 2.45% decrease in male

prevalence.

In addition, comparison of the baseline values for $\gamma_{M,U}$ and $\gamma_{F,U}$ indicates that the population of male users present the most obvious gender-behavior group for prevention measures with regard to the cost-benefit of such a public health intervention. This claim is supported by the baseline value's position near the absolute minimum on the sensitivity curve. Additionally, a 1% change in the parameter value in either direction would have a significant impact on the corresponding STI prevalence.

In a similar fashion to the results presented above for $\gamma_{g,U/NU}$, the sensitivity curves of $C_{g_1g_2}^{s_1,s_2}$ indicate $C_{M_F}^{U,U}$ and $C_{F_M}^{U,U}$ have the greatest impact on the prevalence and incidence of STIs, as quantified by the percentage of change in STI prevalence. This finding is logical because increased sexual risk behavior is associated with dating app users and, as such, $C_{M_F}^{U,U}$ and $C_{F_M}^{U,U}$ are postulated to have a larger impact on the prevalence and incidence of STIs. The corresponding sensitivity curves are shown below.

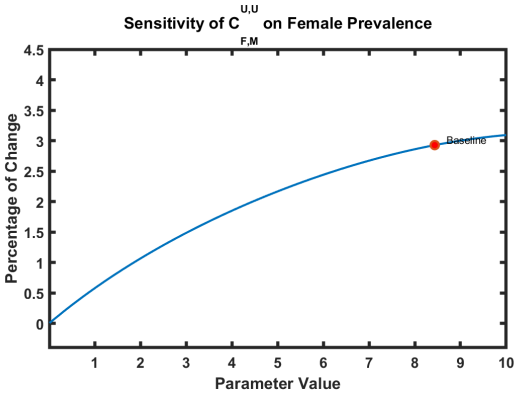

Figure 14: $C_{F_M}^{U,U}$ Female Prevalence

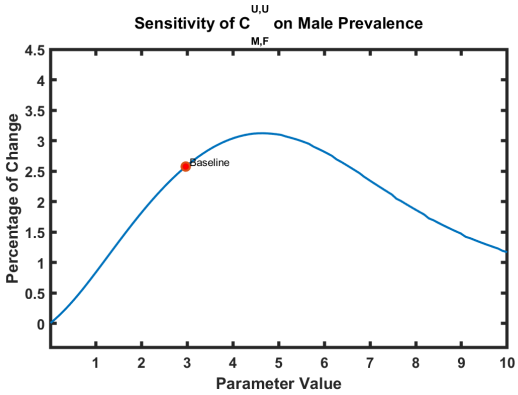

Figure 15: $C_{M_F}^{U,U}$ Male Prevalence

Interpretation of Figure 6 and Figure 7 indicate that a 1% increase in $C_{M_F}^{U,U}$ results in a 2.6% increase in male prevalence whereas a 1% increase in $C_{F_M}^{U,U}$ results in a 2.7% increase in female prevalence. Furthermore, a 1% increase in $C_{M_F}^{U,U}$ suggests a 2.2% increase in female prevalence while a 1% increase in $C_{F_M}^{U,U}$ indicates a 2.5% increase in male prevalence.

The results suggested by the figures above are further supported by comparison of the following two sets of sensitivity curves: (1) $C_{M_F}^{U,NU}$, $C_{M_F}^{U,U}$, $C_{M_F}^{NU,U}$, and $C_{M_F}^{NU,NU}$; and (2) $C_{F_M}^{U,U}$, $C_{F_M}^{U,NU}$, $C_{F_M}^{NU,U}$, and $C_{F_M}^{NU,NU}$. Regarding the former,a 1% increase in $C_{M_F}^{U,U}$ presents the largest increase in male incidence and prevalence rates. Similarly, for latter set a 1% increase in $C_{F_M}^{U,U}$ corresponds to the largest increase in female incidence and prevalence rates.

Synthesis of the sensitivity analyses for γ_g and $C_{g_1g_2}$ reveals that perturbations among the male dating app users results in consistently greater percent changes in the incidence and prevalence of STIs, in comparison to the other sex-behavior classes. From a public health standpoint, this presents male dating app users as the most influential sex-behavior population for an intervention. Based on the data, targeting other sex-behavior groups would not result in as big of impact in the reduction of the incidence and prevalence of STIs.

8.3 PCRA Plots

Partial Rank Correlation Analysis was conducted for the parameters γ_g^s and $C_{g_1g_2}^{s_1s_2}$ and the four pertinent sex-behavior populations. The former is shown in Figure 16.

As shown, the positivity of the correlation coefficient for γ_g^s differs for incidence and prevalence, with prevalence having a negative r value. This negative correlation is logical as a larger γ_g^s corresponds to

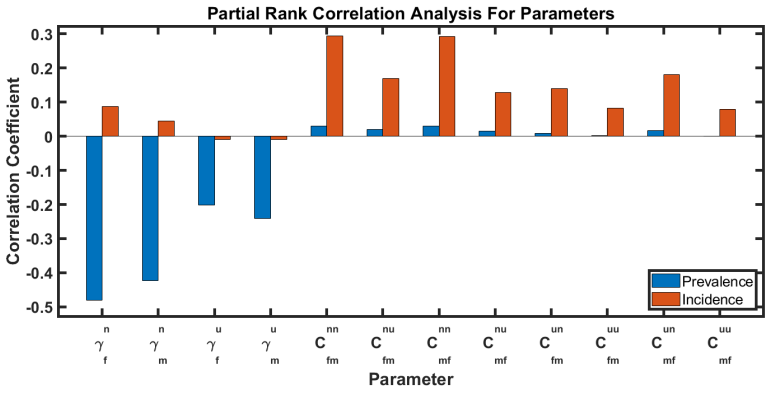

Figure 16: PCRA of Fitted Parameters

a smaller duration of infection for the infected individual. As very small values of γ_g^s are unlikely, the prevalence and γ_g^s are understood to share a negative correlation. In contrast, γ_g^s and incidence present a positive correlation coefficient as larger values of γ_g^s correspond to a larger susceptible class. This phenomenon relies on the incidence being represented by $\lambda S(t)$.

In contrast to γ_g^s, the correlation coefficients for all combinations of $C_{g_1 g_2}^{s_1 s_2}$ and incidence and prevalence are positive values. This suggests that as the unit per capita probability of transmission from sex g_2 to sex g_1 assumes larger values, there is a greater observed incidence and prevalence of STIs. This conclusion is sensible and indicates both the validity and reliability of our model.

Figure 18 exhibits the partial rank correlation analysis for the eight combinations between four pertinent sex-behavior populations and the incidence and prevalence of STIs.

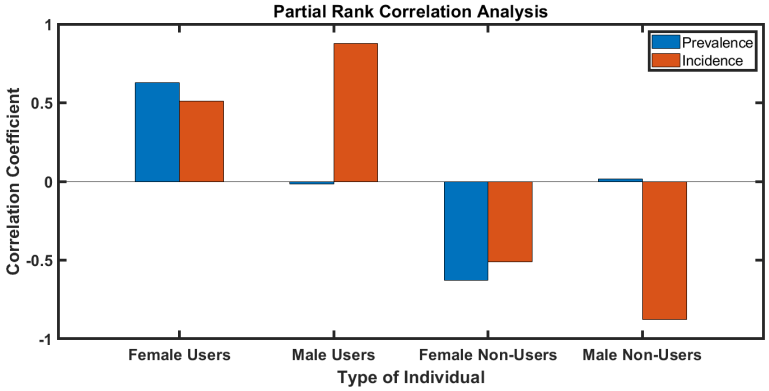

Figure 17: PCRA of Sex-Behavior Category

Regarding the correlation coefficients associated with STI incidence, female and male users demonstrate a positive r value whereas female and male non-users demonstrate a negative. This trend suggests that dating-app users have a greater impact on the annual rate of newly acquired STIs. This is supported by further analysis of the correlation coefficients for male uses and non-users. For instance, for STI incidence male users (r = 0.9) maintain a strong positive correlation and male nonusers a strong negative correlation (r = -0.9). Moreover, sex comparisons among dating app users and non-users present males as having a greater relationship with STI incidence than females from either population. From a public health standpoint, this argues for male users being the target population for intervention strategies.

Figure 18 also provides relationship assessments for STI prevalence in accordance to the four previously discussed sex-behavior categories. For female users and female non-users the moderately strong correlation coefficients (r = 0.6 and -0.6, respectively) are intuitive; STI prevalence increases as the number of female uses increases and decreases as the number of female non-users increases. In contrast, the correlation coefficients for STI prevalence among male users and male non-users are peculiar, however

the have p-values greater than 0.05 and, thus, are not significant. As such, the validity and reliability of our model is preserved.

8.4 Scenario Analysis

Scenario analysis was conducted to assess the potential impact of ad campaigns being implemented into dating apps. Calculations relied upon the reduction of $C_{g_1 g_2}^{s_1 s_2}$, the per capita infectivity from sex g_2 and status s_2 to sex g_1 and status s_1. Results were plotted against "Time (year)" on the horizontal axis and "Number of Infected Individual in Millions" on the vertical axis.

Reduction of C_{fm}^{uu} was calculated and assessed for its impact on male prevalence, male incidence, female prevalence, and female incidence between 2009 and 2021. Results suggested that a reduction in the per capita infectivity from male users to female users had the greatest effect on the percent change in female incidence. An example of the procured scenario analysis graphs for male prevalence is shown below.

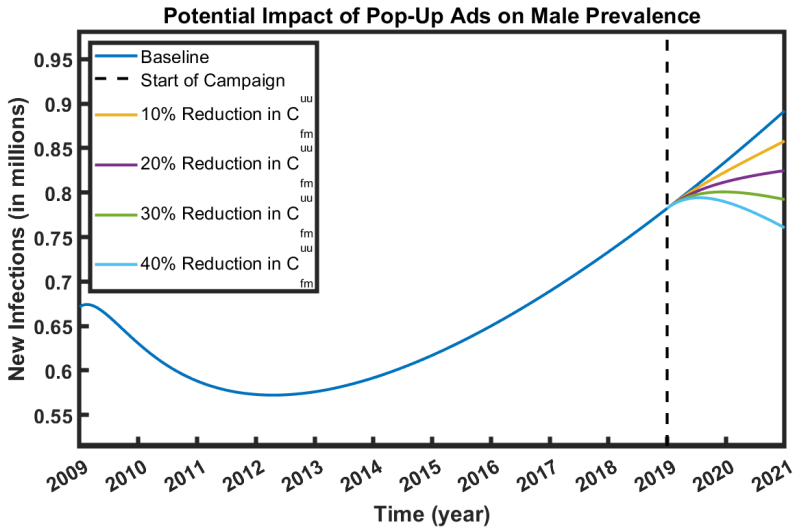

Figure 18: C_{fm}^{uu} Scenario Analysis: Male Prevalence

Table 10 below synthesizes the scenario analyses and provides numeric quantities for the percent change in STI incidence and prevalence that result from a 10%, 20%, 30%, and 40% reduction in C_{fm}^{uu}.

% Reduction in C_{fm}^{uu}	Male Prevalence	Male Incidence	Female Prevalence	Female Incidence
10	4.2	7.3	4.9	7.6
20	7.3	10.9	11.3	15.9
30	11.2	18.2	18.7	23.5
40	14.6	23.6	21.7	29.4

Table 10: C_{fm}^{uu} Scenario Analysis Results

Comparison of the percent change in male and female incidence resulting from a 40% reduction in C_{fm}^{uu} provides salient information regarding the most impactful sex-behavior population to target for a public health intervention. As shown, a 40% reduction in C_{fm}^{uu} results in a 23.6% decrease in male incidence and a 29.4% decrease in female incidence. This indicates that pop-up ads would have the greatest quantifiable effect on female prevalence under the circumstance in which the males transmitted the infection.

Scenario Analysis for C_{mf}^{uu} fails to maintain a similar trend, as displayed in the Table 11 below.

As presented, a 40% reduction in C_{fm}^{uu} results in a 40.0% decrease in male incidence and a 29.4% decrease in female incidence. Thus, a reduction in the transmissibility of infection from male users to

% Reduction in C_{mf}^{uu}	Male Prevalence	Male Incidence	Female Prevalence	Female Incidence
10	4.5	13.6	7.1	7.6
20	12.6	22.7	9.5	14.7
30	22.9	34.5	15.7	22.4
40	28.7	40.9	19.0	29.4

Table 11: C_{mf}^{uu} Scenario Analysis Results

female users has the greatest impact on male prevalence. Synthesized with the projected STI incidence and prevalence corresponding to C_{mf}^{uu}, a the largest percent change in both STI incidence and prevalence occurred for 40% reduction in C_{fm}^{uu}. This finding proposes male users as the most influential population to target for pop-up ads or other related public health campaigns.

In addition to C_{mf}^{uu} and C_{fm}^{uu}, scenario analysis was performed for γ_f^u and γ_m^u. Reduction of γ_g^s signifies an increase in the duration of infection for an infected person which, in turn, decreases the number of susceptible people for the corresponding sex-behavior category. As such, scenario analysis for γ_g^s indicates the quantifiable effect the minimization of the susceptible class has upon STI prevalence and incidence rates.

In comparing γ_f^u and γ_m^u, it is found that reduction of γ_m^u has a greater decrease in female incidence, male incidence, and male prevalence than γ_f^u. This indicates that reducing the per capita recovery rate of male users and, thus, increasing their duration of infection has the greatest potential the sharply increasing rates of STIs in the United States.

9 Conclusion

This study utilized mathematical modeling and statistical analysis to investigate the relationship between dating-app usage and STI incidence and prevalence. Specifically, a four-compartment SIS STI model and an eight-compartment SIS STI model were created reliant on data collected from various sources, but most prominently the CDC and WHO. In conjunction, these models were used to quantify the impact of dating apps upon STI incidence rates and estimate the percentage of people who seek treatment after contracting an STI. Additionally, a modified version of the model allowed for the benefit of in-app prevention campaigns to be assessed.

The four-compartment two-sex SIS STI model was constructed primarily to guide the choice of the parameters used in the eight-compartment two-sex dating-app SIS STI model. The model was also used to study the variability of fit with respect to simulation period and specific STI combinations, as well as to assess the correspondence between the model output and the incidence data.

Concerning the primary use of the four-compartment model, parameter fitting was conducted initially for the computationally derived ξ_g and provided λ_g. The obtained values were then used to ascertain the remaining 6 parameters, γ_f, γ_m, C_{fm}, C_{mm}, C_{mf}, and C_{ff} reliant on the available data of STI incidence by sex. Furthermore, the parameter fitting discussed utilized a descent method. To elaborate, initial conditions for the fitted parameters were supplied based on prevalence data computed from literature. The fitting then produced the optimal parameter values by generating values that minimized error.

After necessary parameters were obtained, the R_0, stability threshold, values corresponding to different STI fittings were successfully computed. Ultimately The R_0 values calculated were all greater than one, providing insight into the equilibrium status of the 4-compartment model. A classical threshold condition for the stability of a disease free equilibrium is that the equilibrium is locally asymptotically stable if R_0 is less than one and is unstable if R_0 is greater than one. This means that for the model, the disease free equilibrium is unstable, and that STI Incidence is not dying out. This directly correlates to the literature review collected regarding to continual growth of STI Incidence within the United States.

Following the parameter fitting and validation of the model using R_0, N(t), the population of sexu-

ally active individuals, was further sub-divided into dating app users and non-users. This resulted in the eight-compartment two-sex dating-app STI SIS model. In contrast to the four-compartment model, the eight-compartment model only considered opposite-sex sexual contacts only. This was done as there are significant gaps in the data regarding same-sex sexual partners by dating app usage and also to avoid the use of an additional 8 constants, which would have created computationally erroneous equations for λ_g, the forces of infection. Furthermore, literature suggests that the quantity of same-sex sexual contacts among all sexual contacts is small. As such, it is postulated that disregarding same-sex sexual contacts will have a negligible affect on the study's findings.

The eight-compartment model was used to conduct a series of four simulations that provide useful information regarding our research aims. For reference, these are listed as follows: to quantify the percentage change in STI incidence and prevalence that results from dating app usage, to assess the impact of pop-up ads upon the incidence and prevalence of STIs, and to identify the sex-behavior group most important for a public-health intervention. Before conducting the simulations, γ_g^s and $C_{g_1g_2}^{s_1s_2}$ were estimated through parameter fitting. The fitting followed the same method as was used for the four-compartment model discussed above.

The first set of these simulations was shown in Figures 6 through 9. From analysis of these four figures, its concluded that both STI incidence and prevalence for females and males has increased annually between 2015 and 2019 and is projected to stabilize at a positive value indicating that STI incidence and prevalence will continue to increase in the future. Moreover, the figures indicate that there is an annual 9-15% increase in male and female prevalence due to dating apps.

Sensitivity analysis for γ_g and $C_{g_1g_2}$ provide information regarding the most influential sex-behavior population with respect to a public health intervention. Regarding $C_{g_1g_2}$, $C_{f_m}^{u,u}$ and $C_{m_f}^{u,u}$ correspond with the greatest percent change in the prevalence and incidence of STIs. As such, users of dating apps are presented as having more impact on the rising STI rates in the United States. This claim is furthered by the sensitivity analysis for γ_g; a 1% increase in γ_f^u and γ_m^u were shown to have the greatest percent change in the incidence and prevalence of STIs. Furthermore, among γ_f^u and γ_m^u, γ_m^u has the greatest decrease in male and female prevalence. As such, it can be stated with reasonable confidence that male users are the sex-behavior group to target for a public health intervention.

Concerning a public health intervention, scenario analysis for γ_g^s and $C_{g_1g_2}^{s_1s_2}$ quantified the impact of prevention campaigns, providing that such an intervention reduces the per capita infectivity from sex g_2 and status s_2 to sex g_1 and status s_1, which is represented by $C_{g_1g_2}^{s_1s_2}$. Table 8 and Table 9 convey that the greatest reduction in STI incidence and prevalence occurs for male prevalence under the condition of a 40% reduction in $C_{f_m}^{uu}$. The datum confirms results from the sensitivity analysis which proposes male dating app users as the sex-behavior group of interest with regards to a prevention campaign.

Partial Rank Correlation Analysis for γ_g^s and $C_{g_1g_2}^{s_1s_2}$ and the four pertinent sex-behavior populations further confirms male users as the target group for in-app prevention campaigns. As shown in Figure 15, the relationship between male dating-app users and STI incidence maintains the correlation coefficient of the largest positive magnitude. Correspondingly, the relationship between male dating-app non-users and STI incidence maintains the correlation coefficient of the largest negative magnitude. These statistics further indicate male users as the sex-behavior group of interest with regard to a public health intervention campaign.

In addition to the four simulations, the eight-compartment SIS model was used to compute the duration of infection for an infected individual. This computation relied upon Equation 3, solving for $\frac{1}{\gamma_g}$, as presented in the "Parameter Fitting for the 4-Compartment SIS Model" section. After finding literature values for 5 out of the 7 parameters, a functional dependence graph was created for σ and θ. Analysis of this relationship indicates that the percentage of identified infections is likely very high, between 90% and 97%.

Overall, the two SIS models for STIs and their associated computations, parameter fittings, and simulations provided significant information concerning the relationship between dating apps and STIs and, additionally, supplied novel STI prevalence data. Reliant on data from the simulations, it was

found that there is a significant increase in STI prevalence and incidence due to dating apps, with the annual increase in male and female prevalence due to dating apps being between 9% and 15%. Moreover, algebraic computation of Equation 3 found that the percent of infected individuals who seek treatment is likely between 90% and 97%.

Concerning a public health intervention, scenario analysis for γ_g^s and $C_{g_1 g_2}^{s_1 s_2}$ indicates that pop-up ads have a quantifiable effect on the reduction of STI incidence and prevalence. This signifies that in-app prevention campaigns are note-worthy mediation strategy to reduce the prevalence and incidence of STIs from continuing to rise. Furthermore, regarding public health, results from the scenario analysis, sensitivity analysis, and PCRA plots suggest male app users as the group to target for a prevention campaign as they are the group with the largest impact on STI prevalence and incidence.

10 Acknowledgments

The authors thank the National Science Foundation for award DMS #2150492, and the Office of the Dean of The College of Liberal Arts and Sciences at Arizona State University for funding this research.

References

[1] J. C. Abma and G. M. Martinez. "Sexual Activity and Contraceptive Use Among Teenagers in the United States, 2011-2015". In: 104 (2017), pp. 1–23.

[2] C. L. Althaus et al. "Transmission of Chlamydia trachomatis through sexual partnerships: a comparison between three individual-based models and empirical data". In: *Journal of the Royal Society, Interface* 9 (66 Jan 7 2021), pp. 136–46. DOI: 10.1098/rsif.2011.0131.

[3] Elizabeth Arias, Melonie Heron, and Jiaquan Xu. "United States Life Tables, 2014". In: *National Vital Statistics Reports* 66.4 (August 14, 2017).

[4] Ryan A. Bable and Julie Ackerlund Brandt. "Delay Discounting, Dating Applications, and Risky Sexual Behavior: An Exploratory Study". In: *The Psychological Record* 72 (Jan. 2022), pp. 1–6. DOI: 10.1007/s40732-021-00506-6.

[5] Patricia A. Cavazos-Rehg et al. "Age of sexual debut among US adolescents". In: *Contraception* 80 (2 Aug. 2009), pp. 158–62. DOI: 10.1016/j.contraception.2009.02.014.

[6] Centers for Disease Control and Prevention. *Chlamydia treatment and care*. Division of STD Prevention, National Center for HIV, Viral Hepatitis, STD, and TB Prevention, Centers for Disease Control and Prevention, July 22, 2021. Accessed 07-12-2023. URL: https://www.cdc.gov/std/chlamydia/treatment.htm.

[7] Centers for Disease Control and Prevention. "Incidence, Prevalence, and Cost of Sexually Transmitted Infections in the United States". In: *Fact Sheets* (2022). URL: https://www.cdc.gov/nchhstp/newsroom/fact-sheets/std/STI-Incidence-Prevalence-Cost-Factsheet.htm.

[8] Anjani Chandra et al. "Sexual Behavior, Sexual Attraction, and Sexual Identity in the United States: Data From the 2006-2008 National Survey of Family Growth". In: *National Health Statistics Reports* 36 (March 3, 2011).

[9] S. Dixon. *U.S. smartphone dating app users 2019-2023*. Statista, April 28, 2022. Accessed 07-12-2023. URL: https://www.statista.com/statistics/274144/smartphone-dating-app-users-usa/.

[10] P. van den Driessche and J. Watmough. "Reproduction numbers and sub-threshold endemic equilibria for compartmental models of disease transmission. Mathematical biosciences". In: *Mathematical Biosciences* 180 (2002), pp. 29–48. DOI: https://doi.org/10.1016/s0025-5564(02)00108-6.

[11] Bethany G. Everett. "Sexual orientation disparities in sexually transmitted infections: examining the intersection between sexual identity and sexual behavior". In: *Archives of sexual behavior* 42 (2013), pp. 225–236.

[12] Thomas A. Farley, Deborah A. Cohen, and Whitney Elkins. "Asymptomatic sexually transmitted diseases: the case for screening". In: *Preventive Medicine* 36.4 (2003), pp. 502–509. URL: https://www.sciencedirect.com/science/article/pii/S0091743502000580.

[13] Jon Fortenbury. "On 'Late'-In-Life Virginity Loss". In: *The Atlantic* (2014). URL: https://www.theatlantic.com/health/archive/2014/03/on-late-in-life-virginity-loss/284412/.

[14] Lori Gorshow. "Helpful Advice for a 30 Year Old Virgin". In: *Love to Know* (September 27, 2018). URL: https://www.lovetoknow.com/life/relationships/30-year-old-virgin.

[15] Joanna M. Kesten et al. "Acceptability and potential impact of delivering sexual health promotion information through social media and dating apps to MSM in England: a qualitative study". In: *BMC Public Health* 19 (2019), pp. 1–9.

[16] R. D. Kirkcaldy et al. "Epidemiology of gonorrhoea: a global perspective". In: *Sex Health* 16 (5 Sep 2019), pp. 401–411. DOI: 10.1071/SH19061.

[17] Madeline Lenahan. *Dating app engagement surpasses pre-pandemic levels*. apptopia, December 4, 2020. Accessed 07-12-2023. URL: https://blog.apptopia.com/dating-app-engagement-has-surpassed-pre-pandemic-levels.

[18] M. Martín-Sánchez et al. "Clinical presentation of asymptomatic and symptomatic women who tested positive for genital gonorrhoea at a sexual health service in Melbourne, Australia". In: *PubMed Central* (2020).

[19] Gladys M. Martinez and Joyce C. Abma. "Sexual Activity and Contraceptive Use Among Teenagers Aged 15–19 in the United States, 2015–2017". In: *NCHS Data Brief* 366 (May 2020).

[20] Monica Molano et al. "The natural course of Chlamydia trachomatis infection in asymptomatic Colombian women: a 5-year follow-up study". In: *Journal of Infectious Diseases* 191 (2005), pp. 907–916.

[21] Tom Morris. *Dating in 2021: swiping left on COVID-19*. Global Web Index, March 2, 2021. Accessed 07-12-2023. URL: https://blog.gwi.com/chart-of-the-week/online-dating/.

[22] National Committee for Quality Assurance. *chlamydia screening in women*. NCQA. Accessed 07-12-2023. URL: //www.ncqa.org/hedis/measures/chlamydia-screening-in-women/.

[23] Ashlee N. Sawyer, Erin R. Smith, and Eric G. Benotsch. "Dating application use and sexual risk behavior among young adults". In: *Sexuality Research and Social Policy* 15 (2018), pp. 183–191.

[24] Cruz Vargas de León. "On the global stability of SIS, SIR and SIRS epidemic models with standard incidence". In: *Chaos, Solitons & Fractals* 44 (12 December 2011), pp. 1106–1110.

[25] Hillard S. Weinstock et al. "STI prevalence, incidence, and costs in the United States: New estimates, new approach". In: *Sexually Transmitted Diseases* 48.4 (2021), p. 207.

[26] World Health Organization. "Sexually transmitted infections (STIs)". In: *Fact Sheets* (2022). URL: https://www.who.int/news-room/fact-sheets/detail/sexually-transmitted-infections-(stis).